Image-Based Structural Health Monitoring Methodology for Corrosion Diagnosis and Prognosis

LUCIO PINELLO, DAYOU MA, LOURDES VAZQUEZ-GOMEZ, LUCA MATTAROZZI, ALESSANDRO BENEDETTI, ANDREA BALDI, UGO MARIANI, MARCO GIGLIO, ANDREA MANES and CLAUDIO SBARUFATTI

ABSTRACT

Corrosion is a serious concern for structural integrity since it can lead to premature structural failures. Nevertheless, its monitoring is particularly challenging due to inherent features of the corrosion process: it is strongly dependent on environmental conditions, materials used, and their coupling. Generalised corrosion phenomena are visible at visual inspection and lead to a reduction of the resistant thickness of components and structures. Instead, localised corrosion results in visually difficult-to-detect damages that can lead to fatigue cracks. In addition, these two corrosion types are not mutually exclusive: a component may present corrosion pits even if it is macroscopically subjected to generalised corrosion. However, a probability-based relationship between generalised corrosion evolution and corrosion pits' presence and geometrical features is missing. Therefore, it is important to monitor generalised corrosion phenomena to assess the structural integrity of structures and components given the reduction in their resistant section and the possible presence of corrosion pits. Within this context, this study presents a methodology for corrosion-based structural assessment by integrating image-based corrosion diagnosis, measurements of environmental and corrosion rate related parameters, and a filtering technique to perform corrosion diagnosis and prognosis. The image-based corrosion diagnosis relies on a Convolutional Neural Network (CNN) that has been trained to automatically perform semantic segmentation on images of a corroded helicopter component. In this way, it is possible to have discrete-in-time observations of the actual corrosion level of the component when the helicopter is not on missions. The implemented CNN is not only able to distinguish between corroded and uncorroded regions but also between two different corroded regions of interest due to different materials. The CNN was trained with manually segmented images from which corrosion indexes have been extracted. The latter have been related to (i) environmental parameters and (ii) corrosion rate related parameters. In this way, two models have been obtained offline to predict corrosion evolution. Eventually, a Particle Filter (PF) was implemented to adapt the models to the observations of the corrosion level by the CNN. The proposed framework integrates image processing, sensor measurements, and filtering techniques for structural assessment. The PF guarantees the adaptability to real-time observations of the corrosion evolution models developed offline, improving the reliability of the methodology. While the presented framework has been applied to a helicopter component, it can be easily applied to other systems. For instance, being based on image processing, its image-based nature makes it well-suited for monitoring offshore or hard-to-access structures using drones or fixed cameras. Eventually, this study provides a step towards a more accurate and data-driven corrosion prognosis, enhancing the accuracy of structural integrity assessments.

*

INTRODUCTION

Corrosion monitoring is a critical aspect due to its intrinsic probabilistic nature and the intricate interplay between environmental factors and the material under corrosion. Corrosion endangers the structural component integrity by reducing their thickness and favouring the initiation of crack nucleation sites [1,2], as in the case of pitting corrosion. A key feature of the corrosion process is that the corrosive phenomena are not mutually exclusive, therefore it is possible to have pitting corrosion in a macroscopic generalised corrosion. However, no probability-based relationship between generalised corrosion and corrosion pits presence exists.
Within the Structural Health Monitoring (SHM) framework, corrosion phenomena are usually monitored by exploiting non-destructive techniques (NDT) [3–6]. However, NDTs are only able to diagnose the current state of corrosion. Therefore, machine learning (ML) techniques are being developed and implemented for SHM purposes to predict the corrosion rate of different phenomena [7–10].
Therefore, this work proposes a generalised corrosion monitoring framework to assess the structural integrity of structures and components considering the possible presence of corrosion pits. The framework relies on an image-based corrosion diagnosis step and a prognostic step. Image-based corrosion diagnosis relies on a Convolutional Neural Network (CNN) to perform semantic segmentation on images of a corroded helicopter component (HC). These are discrete-in-time observations of the actual HC corrosion level when the helicopter is not on missions. The CNN was trained with manually segmented images from which corrosion indexes have been extracted. The latter have been related to measures of either environmental parameters or corrosion-rate related parameters, obtaining two models for corrosion evolution prediction. The prognostic step uses the models developed in a Particle Filter (PF), which also enables the adaptation of the models to the CNN's actual corrosion level measurements. The PF guarantees the adaptability to real-time observations of the corrosion evolution models developed offline, improving the reliability of the methodology.
The proposed framework integrates image processing, sensor measurements, and filtering techniques for structural assessment. Its image-based nature makes it well-suited for monitoring offshore or hard-to-access structures using drones or fixed cameras.
Eventually, this study provides a step towards a more accurate corrosion prognosis, improving the accuracy of structural integrity assessments.

METHODOLOGY

This section describes the methodology implemented for the image-based SHM methodology for corrosion diagnosis and prognosis.
The framework developed relies on four steps to assess the structural assessment: (i) models building and CNN training, (ii) corrosion diagnosis and prognosis, (iii) predictions updating when new measurements are available, and (iv) inspection intervals up-

Lučio Pinello, PhD Student, Email: lucio.pinello@polimi.it. Department of Mechanical Engineering, Politecnico di Milano, Milan, MI, Italy.

dating by estimating the Residual Useful Life (RUL) based on corrosion level. The first step of the framework must be performed offline, while the remaining three work online. The offline step consists of (i) manual segmentation of corroded HC images, (ii) extraction of corrosion indexes (D) from the segmented images, (iii) training of the CNN on manually segmented images to perform automatic segmentation, and (iv) models based on D and measurements acquired during exposure of the HCs. Segmentation means associating a label to each pixel of an image, and the available pixel labels are *HC* and *corrosion*. Figure 1 shows semantic segmentation applied to a generic corroded plate.
The damage indexes D are evaluated as the ratio between the number of pixels associated with HC corrosion and the total number of pixels of the image. Then, a fitting was performed to relate D to (i) the corrosion-evolution related parameters measured by a sensor and (ii) the cumulatives of temperature, humidity and chloride salt deposition obtained from a weather ground-station. The cumulatives have been used to take into account time exposure. The cumulative of the free corrosion charge is not needed since it is defined as the integral of the current over time, so time exposure is already addressed. The choice between the two models only depends on data, e.g., sensor, availability.
Eventually, the CNN can be trained to perform automatic semantic segmentation, that is, automatic labelling of image pixels to distinguish between corroded and non-corroded regions. Once the CNN is trained and models have been built, the real-time operational phase takes place. It relies on real-time measurements of either corrosion-related or environmental parameters that serve as input to the models developed offline to estimate the corrosion level (D_m) of the HC during helicopter missions. Then, when the helicopter goes back to the warehouse, pictures of the HC can be taken and fed to the CNN for automatic segmentation. The CNN gives as output the actual corrosion level (D_{seg}) of the HC and this observation of the real corrosion level is used in a PF to correct the latest model prediction D_m, obtaining the updated prediction and prognosis of the corrosion level D_m^*. Eventually, the inspection interval can be updated by knowing the corrosion evolution prediction. In addition, if one knows the probability of having a corrosion pit, and its geometrical properties, given a certain level of generalised corrosion, it is also possible to compute the RUL of the HC evaluating if the pit propagates mechanically as a fatigue crack. However, this last step depends on the specific component under analysis and lacks of research interest. Therefore, it is not included in this work.

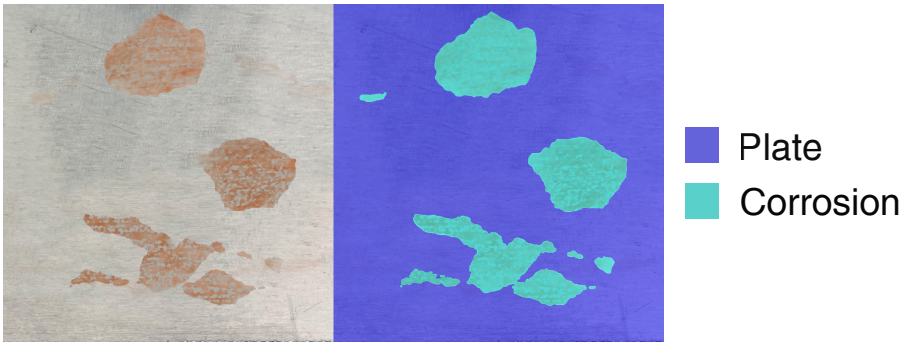

Figure 1. Example of semantic segmentation on a generic plate.

CASE STUDY

Three identical HCs were exposed to a marine environment at the CNR MARECO facility in Bonassola (Italy) from 06/05/2022 to 10/03/2024, namely HC-1, HC-2, and HC-3. The HCs were photographed at different exposure times,e.g., different corrosion levels, for a total of 22 images, e.g., one per month. At the same time, a LUNA ACUITY LS sensor [11] was exposed to the same environment. This sensor hosts a lamina of the same material as HC and measures, among environmental parameters, the free corrosion charge. The focus is set only on the free corrosion charge for the LUNA ACUITY LS sensor since it directly describes the evolution of the corrosion process from the electrochemical point of view, including the effects that temperature, humidity, and other parameters have on it. Similarly, temperature and humidity variations and chloride deposition concentrations were acquired from an environmental ground station close to the MARECO facility and with an on-ground salt-deposition trap in the MARECO facility, respectively. Starting with the offline phase of the framework, the HCs' pictures were manually segmented to distinguish between corroded and non-corroded regions of the component. An FCN-8s [12] network has been implemented to perform semantic segmentation, and its architecture is shown in Table I. The training has been performed on two of the four HCs, namely HC-1 and HC-2. The same two HCs were used to build the two models for the evolution of the corrosion index. Figure 4 and Figure 5 show the corrosion indexes obtained by fitting the corrosion indexes D extracted from manual segmentation with cumulative of environmental parameters ($D_{m,env}$) and free-corrosion charge ($D_{m,chr}$), respectively. Operatively, the choice between the two models depends only on sensor availability since it is preferable to use the model based on the free corrosion charge since the sensor measuring this quantity must be installed directly on the helicopter. Therefore, it measures a parameter related to the actual operating conditions of the HC. Instead, the environmental parameters may be related to locations that can differ from the local operating conditions of helicopter missions. However, thanks to the PF, the choice of the model affects only partially the goodness of the prediction since it is possible to adapt the prognosis to observation of the actual corrosion level.

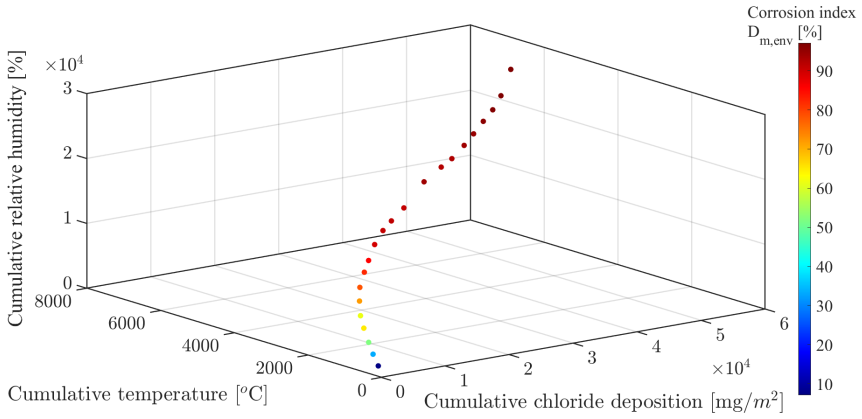

Figure 2. Corrosion indexes $D_{m,env}$ obtained with the model based on environmental data.

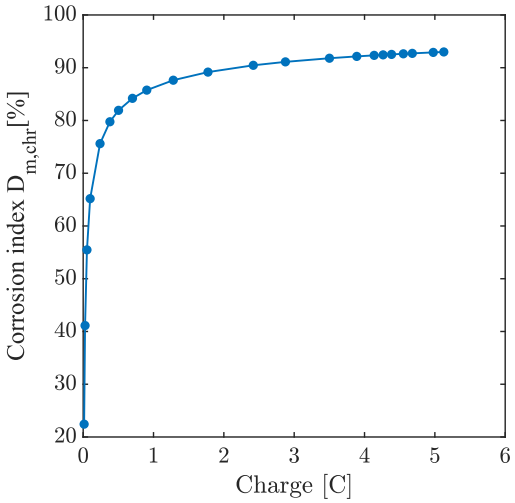

Figure 3. Corrosion indexes $D_{m,chr}$ obtained with the model based on free corrosion charge data.

Moving on to online operations, these models allow for continuous monitoring during operations of the corrosion level, while the automatic segmentation of the HC pictures represents a discrete assessment of the actual corrosion level when the helicopter goes back to the warehouse. Figures 4 and 5 show an example of a real-time operation on HC-3 using the models based on environmental parameters and free-corrosion charge, respectively. The blue lines and triangles represent the average of the corrected prediction given the observation (HC segmentation) made at the k-th step, while the black lines represent the confidence bounds on the corrected predictions. The yellow triangle shows the initial estimation of the corrosion index. Instead, the coloured curves in Figure 4a and Figure 5a represent particles' propagation, showing the prognosis and its statistical dispersion. The figures show that both models can be successfully adapted to observations of the actual corrosion level thanks to the PF algorithm. However, it is not easy for the PF to adapt the models to either a constant or decreasing trend of the corrosion index. This is due to the growing trends shown by the developed model, e.g., the process equations implemented in the PF. Indeed, this is not the trend expected from corrosion evolution. The trend shown by the corrosion indexed observed with the semantic segmentation is due to an intentional cleaning of the surface of the HC-3. The cleaning removed the oxidation product formed on HC-3's surface, causing observed decreasing and constant trends. Therefore, the cleaning operations allowed for a stress test of the developed framework with challenging data.

Layer	Type	Kernel	Stride	Padding	Output Shape
Conv1-1	Conv2D	3×3	1	1	$H \times W \times 64$
Conv1-2	Conv2D	3×3	1	1	$H \times W \times 64$
Pool1	MaxPool2D	2×2	2	0	$H/2 \times W/2 \times 64$
Conv2-1	Conv2D	3×3	1	1	$H/2 \times W/2 \times 128$
Conv2-2	Conv2D	3×3	1	1	$H/2 \times W/2 \times 128$
Pool2	MaxPool2D	2×2	2	0	$H/4 \times W/4 \times 128$
Conv3-1	Conv2D	3×3	1	1	$H/4 \times W/4 \times 256$
Conv3-2	Conv2D	3×3	1	1	$H/4 \times W/4 \times 256$
Conv3-3	Conv2D	3×3	1	1	$H/4 \times W/4 \times 256$
Pool3	MaxPool2D	2×2	2	0	$H/8 \times W/8 \times 256$
Conv4-1	Conv2D	3×3	1	1	$H/8 \times W/8 \times 512$
Conv4-2	Conv2D	3×3	1	1	$H/8 \times W/8 \times 512$
Conv4-3	Conv2D	3×3	1	1	$H/8 \times W/8 \times 512$
Pool4	MaxPool2D	2×2	2	0	$H/16 \times W/16 \times 512$
Conv5-1	Conv2D	3×3	1	1	$H/16 \times W/16 \times 512$
Conv5-2	Conv2D	3×3	1	1	$H/16 \times W/16 \times 512$
Conv5-3	Conv2D	3×3	1	1	$H/16 \times W/16 \times 512$
Pool5	MaxPool2D	2×2	2	0	$H/32 \times W/32 \times 512$
FC6	Conv2D	7×7	1	0	$H/32 \times W/32 \times 4096$
FC7	Conv2D	1×1	1	0	$H/32 \times W/32 \times 4096$
Score Pool5	Conv2D	1×1	1	0	$H/32 \times W/32 \times C$
Upsample 1	Deconv2D	4×4	2	1	$H/16 \times W/16 \times C$
Score Pool4	Conv2D	1×1	1	0	$H/16 \times W/16 \times C$
Upsample 2	Deconv2D	4×4	2	1	$H/8 \times W/8 \times C$
Score Pool3	Conv2D	1×1	1	0	$H/8 \times W/8 \times C$
Upsample 3	Deconv2D	8×8	8	0	$H \times W \times C$

TABLE I. FCN-8s Architecture.

CONCLUSIONS

This work presented an image-based framework for corrosion diagnosis and prognosis. The workflow of the proposed framework can be resumed in the following steps:

1. Manual segmentation of images of HC at different corrosion levels and extraction of corrosion indexes.

2. Corrosion evolution models generation by fitting corrosion indexes with sensor measurements.

3. CNN training to perform automatic semantic segmentation.

4. Corrosion diagnosis and prognosis with predictions updating when component images are available.

5. Inspection interval updating based on corrosion level prognosis.

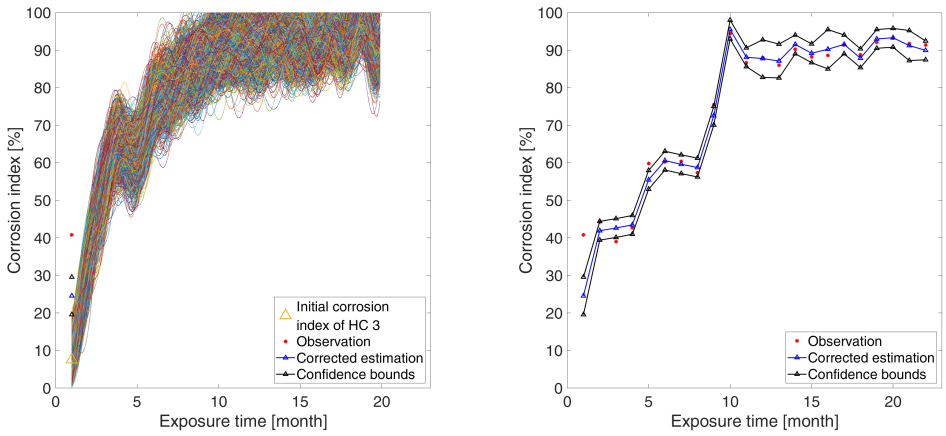

(a) (b)

Figure 4. Results of the PF applied to the model based on environmental parameters after (a) 1 and (b) 22 months of exposure. The coloured curves in (a) represent particles' propagation, showing the prognosis and the statistical dispersion.

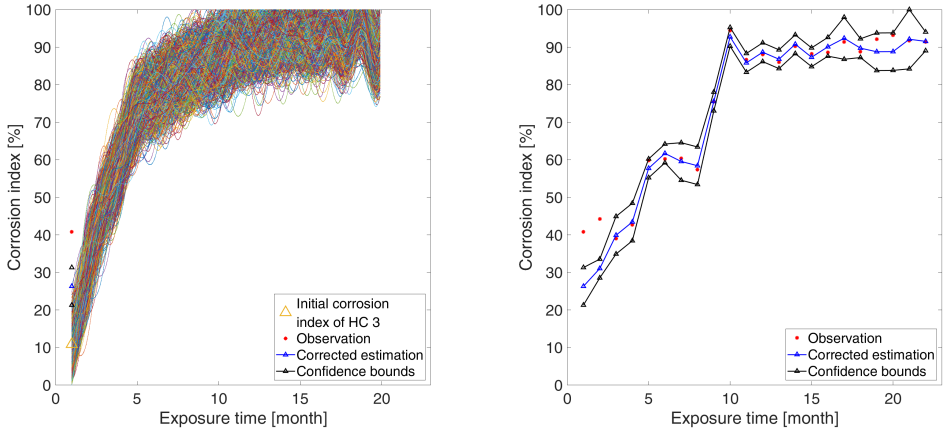

(a) (b)

Figure 5. Results of the PF applied to the model based on free-corrosion charge after (a) 1 and (b) 22 months of exposure. The coloured curves in (a) represent particles' propagation, showing the prognosis and the statistical dispersion.

The results have shown that the proposed framework successfully allows for corrosion diagnosis and prognosis. The framework is suitable for hard-to-access structures using drones or cameras, thanks to its image-based nature that guarantees flexibility in the application. Future work can focus on the application of transfer learning techniques to adapt the CNN trained for semantic segmentation to new components.

ACKNOWLEDGMENT

This work has been developed based on the results from SAMAS 2 project (Struc-

tural health and ballistic impact monitoring and prognosis on a military helicopter), a Cat.-B project coordinated by the European Defense Agency (EDA) and financed by two nations, Italy and Poland. The project consortium includes the following parties: Italy (Politecnico di Milano, Leonardo S.p.A. - Helicopter Division, Consiglio Nazionale delle Ricerche) and Poland (Instytut Techniczny Wojsk Lotniczych - AFIT, Military Aviation Works No. 1, Institute of Aviation, Military University of Technology).

REFERENCES

1. Horner, D., B. Connolly, S. Zhou, L. Crocker, and A. Turnbull. 2011. "Novel images of the evolution of stress corrosion cracks from corrosion pits," *Corrosion Science*, 53(11):3466–3485, ISSN 0010-938X, doi:https://doi.org/10.1016/j.corsci.2011.05.050.
2. Turnbull, A., L. Wright, and L. Crocker. 2010. "New insight into the pit-to-crack transition from finite element analysis of the stress and strain distribution around a corrosion pit," *Corrosion Science*, 52(4):1492–1498, ISSN 0010-938X, doi:https://doi.org/10.1016/j.corsci.2009.12.004.
3. Morizet, N., N. Godin, J. Tang, E. Maillet, M. Fregonese, and B. Normand. 2016. "Classification of acoustic emission signals using wavelets and Random Forests: Application to localized corrosion," *Mechanical Systems and Signal Processing*, 70-71:1026–1037, ISSN 0888-3270, doi:https://doi.org/10.1016/j.ymssp.2015.09.025.
4. Jomdecha, C., A. Prateepasen, and P. Kaewtrakulpong. 2007. "Study on source location using an acoustic emission system for various corrosion types," *NDT E International*, 40(8):584–593, ISSN 0963-8695, doi:https://doi.org/10.1016/j.ndteint.2007.05.003.
5. Homborg, A., T. Tinga, X. Zhang, E. van Westing, P. Oonincx, J. de Wit, and J. Mol. 2012. "Time–frequency methods for trend removal in electrochemical noise data," *Electrochimica Acta*, 70:199–209, ISSN 0013-4686, doi:https://doi.org/10.1016/j.electacta.2012.03.062.
6. Hoseinieh, S., A. Homborg, T. Shahrabi, J. Mol, and B. Ramezanzadeh. 2016. "A Novel Approach for the Evaluation of Under Deposit Corrosion in Marine Environments Using Combined Analysis by Electrochemical Impedance Spectroscopy and Electrochemical Noise," *Electrochimica Acta*, 217:226–241, ISSN 0013-4686, doi:https://doi.org/10.1016/j.electacta.2016.08.146.
7. Qian, H. Z. . T. M., G. 2024. "Diagnostics and Prognostics of Pitting Corrosion in Large Civil infrastructure Using Multi-scale Simulation and Machine Learning," in *Proceedings of the 10th European Workshop on Structural Health Monitoring (EWSHM 2024)*, doi:https://doi.org/10.58286/29734.
8. Luchun Yan, Z. L., Yupeng Diao and K. Gao. 2020. "Corrosion rate prediction and influencing factors evaluation of low-alloy steels in marine atmosphere using machine learning approach," *Science and Technology of Advanced Materials*, 21(1):359–370, doi:10.1080/14686996.2020.1746196, pMID: 32939161.
9. De Masi, G., M. Gentile, R. Vichi, R. Bruschi, and G. Gabetta. 2015. "Machine learning approach to corrosion assessment in subsea pipelines," in *OCEANS 2015 - Genova*, pp. 1–6, doi:10.1109/OCEANS-Genova.2015.7271592.
10. Ossai, C. I., B. Boswell, and I. Davies. 2016. "Markov chain modelling for time evolution of internal pitting corrosion distribution of oil and gas pipelines," *Engineering Failure Analysis*, 60:209–228, ISSN 1350-6307, doi:https://doi.org/10.1016/j.engfailanal.2015.11.052.
11. Luna Innovations Incorporated. *LUNA ACUITY LS - Corrosion Monitoring System*.
12. Long, J., E. Shelhamer, and T. Darrell. 2015. "Fully convolutional networks for semantic segmentation," in *2015 IEEE Conference on Computer Vision and Pattern Recognition (CVPR)*, pp. 3431–3440, doi:10.1109/CVPR.2015.7298965.